The Dynamic Stress State of the Wheel-Rail Contact

XIN ZHAO [*], ZILI LI [*], COENRAAD ESVELD [*], ROLF DOLLEVOET [#]
[*]Section of Road and Railway Engineering, Faculty of Civil Engineering and Geosciences
Delft University of Technology
Stevinweg 1, 2628 CN Delft
THE NETHERLANDS
Http://www.rail.tudelft.nl
[#]Infra Management Railsystems, Department of Civil Technology, ProRail
P.O. Box 2038, 3500 GA Utrecht
THE NETHERLANDS

Abstract: The rolling contact between wheels and rails is one of the key areas of studies in railway. Nowadays, the rolling contact fatigue (RCF) of rails, especially the surface-initiated RCF, is becoming one of the major concerns in the railway industry. In order to study the initiation and growth of RCF, the stress and strain states of the rails, particularly in the contact interface, have to be predicted accurately. In this paper, a three-dimensional dynamic vehicle-track finite element (FE) model has been created to investigate the dynamic stress state of the rail surface and the effects of the tangential contact force. The model is composed of the primary suspension of vehicle, half locomotive wheelset, one rail, rail pads, and ballast. The wheelset and the rail are modeled using constant stress solid element; the carbody and bogie sprung mass are lumped into one rigid body with suspension; the sleepers are modeled as lumped mass; the fastening and the ballast are modeled as springs and dampers. In addition, the bilinear isotropic elastic-plastic material is used in the rail contact surface, and an explicit integration method is used to solve the problem in the time domain. The results show that the dynamic effects are significant, even in the case with smooth rail contact surface, and the tangential force can greatly increase the shear stress level of the rail surface and reduce the oscillations of the contact stress.

Key-words: Contact mechanics, Rolling contact, Dynamics, Finite element method, Stress

1 Introduction

In studies of railway, wheel-rail rolling contact is one of the main issues. The contact forces developed in the contact are the most important external inputs to the vehicles and the track, and are also the direct cause of the damage of wheels and rails like wear, corrugation, fatigue and fracture. In recent years, with the continuous increase of the running speed and the axle load, the influence of the contact forces on the wheel-rail damage and the track deterioration has received more and more attention. Dynamic rolling contact has therefore attracted great interests.

Although contact mechanics is dated back as early as 1882 with the advent of Hertz theory, the first treatment of rolling contact was done by Cater in the 1920s [1]. He handled the wheel and the rail as two half-spaces and the wheel as a cylinder for boundary conditions, so the contact area was rectangular. Johnson extended Carter's two-dimensional theory to a three-dimensional case of two rolling spheres in which the longitudinal and the lateral creepages were included, but the spin creep was not considered [2]. Further, Vermeulen and Johnson extended the theory for arbitrary smooth surface to the pure creepage without the spin creep [3].

Kalker [4] solved the three-dimensional frictional contact problems with arbitrary magnitudes of the creepages and the spin using a number of numerical methods developed by himself. The solution is basically of boundary element characteristics, and with Boussinesq[5]-Cerruti[6] formula for the influence number. The contact area can be any planar shape.

The above-mentioned solutions are all based on the half-space approximation, and exclude the plasticity of the material and the dynamic effects of the system. In order to handle non-planar contact, such as encountered between the wheel flange root and the rail gage corner, Li [7] extended Kalker's solution into the quasi-quarter space, and applied it to the wear simulation of wheel-rail contact, particularly the severe wear at the wheel flange and the rail gage corner.

Except the contact theories mentioned above, there is another powerful tool for solving contact problem — finite element (FE) method. With FE

model, impact, dynamic effects of the system, multiple-point contact and the micro-roughness of contact surface can all be taken into account [8-11].

Since the 1980s there have been two major types of RCF found worldwide: head checks and squats [12], as illustrated in Fig.1. In analyzing their initiation and growth, the stress and strain states in the contact interface and the subsurface continua have to be determined accurately. To such end a FE model, which takes into account not only the friction and the geometry but also the plasticity and the dynamic effects, has been developed to identify the root causes of squats [13]. Based on the model, the dynamic stress state of wheel-rail contact with dry friction is discussed in this paper.

(a) Head checks

(b) A squat

Fig. 1 RCF in field

2 Model description

This paper focuses on the rolling contact between a wheel and a rail, half vehicle-track system has been modeled only in the vertical direction [12, 13]. The schematic diagram of the model is shown in Fig.2. The *Z*-axis is defined along the longitudinal direction (the rolling direction of the wheel).

The position of the wheel shown in Fig.2 is the starting position of the simulations. The carbody and bogie sprung mass are lumped into one rigid body Mc connected to the wheel with suspension springs Kc and dampers Cc; sleepers are modeled as lumped mass M2; fastening and ballast are modeled as springs K1, K2 and dampers C1, C2. The locomotive wheel with diameter ϕ=1.2 m and the rail (UIC 54), as shown in Fig.3, are modeled using the constant stress solid element. The bilinear isotropic elastic-plastic material is used for the rail contact surface. A 7m length of track is modeled. Very fine mesh is made in the contact zone of the rail in order to get sufficient accuracy. An explicit integration method is used to solve the problem in the time domain. In addition, the penalty function method is used for the contact between the wheel and the rail. The values of some parameters used in the model are listed in Table 1[13-14]. Coulomb friction law is employed and the coefficient of friction is set to 0.3. The rolling speed of the wheel is one of the typical speeds in the Dutch railway network: v=140 km/h.

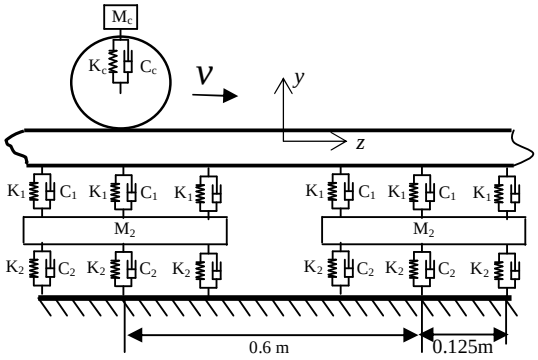

Fig. 2 The schematic diagram of the model

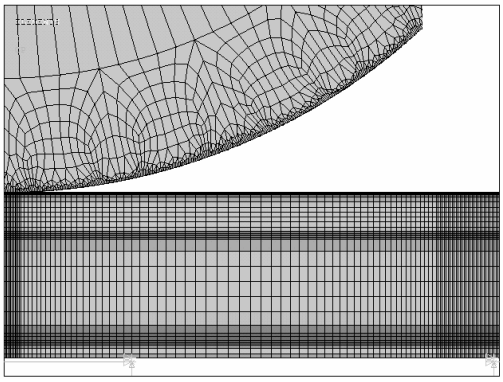

Fig. 3 The FE mesh of the wheel and the rail in contact.

3 Results and discussions

Using the above-mentioned FE model, two rolling cases with different tangential contact force are simulated to study the effects of the tangential contact force. The tangential contact forces in the two cases are

Case 1: $F_T = 0.3F_N$ (1)

Case 2: $F_T = 0.1F_N$ (2)

Where F_T, F_N are the tangential and normal contact forces between the wheel and the rail respectively.

In order to simulate different tangential forces between the wheel and the rail, different drive loads are applied to the wheel shaft.

Table 1, Vehicle, track and material data used

Components	Parameters	Values
Sprung mass	Mass	10,000kg
1st suspension	Stiffness	1.15 MN/m
	Damping	2500 Ns/m
Rail pad	Stiffness	1300 MN/m
	Damping	45 KNs/m
Sleeper	Mass	244 Kg
	Spacing	0.6 m
Ballast	Stiffness	45 MN/m
	Damping	32 KNs/m
Wheel and rail material	Young's modulus	210GPa
	Poisson's ratio	0.3
	Mass density	7,800kg/m^3
	Yield stress	0.8Gpa
	Tangent modulus	21GPa

A contact patch can usually be divided into a slip area and a stick (adhesion) area, as shown in Fig.4. In the slip area, the tangential traction is limited by the Coulomb friction law, and proportional to the contact pressure. According to Hertz theory, the vertical contact force distribution is elliptic. So, if sliding contact happens, the tangential force distribution is also elliptic like $q(z)_m$ shown in Fig 4. For rolling contact, the typical tangential force distribution is like $q(z)$ in Fig.4 [15]. Therefore, the total tangential force increases with the decrease of stick area.

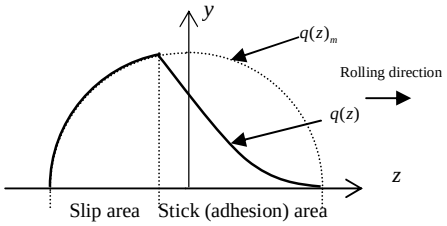

Fig.4 The tangential force distribution in the contact patch

For the case 1 created in this paper, the tangential force F_T reaches the limiting friction force. It is the critical state at the transition between rolling and sliding: the adhesion area may have shrunk into a point, or the wheel is in gross sliding - there is no adhesion area in the contact patch of the case 1, only (micro-) slip exists. The friction between the wheel and the rail was fully utilized for driving. The tangential traction distribution of the case 1 is in the form of $q(z)_m$ in Fig 4. On the contrary, in the case 2, there is not only slip area but also the area of adhesion in the contact patch.

3.1 Comparison with Hertz theory

In order to validate the model, the pressure distribution from the FE model is compared with the Hertz contact theory.

3.1.1 Hertz result

Assuming elastic material, half spaces and small contact patch size for bodies in contact, Hertzian contact theory can be used to predict the wheel/rail pressure distribution.

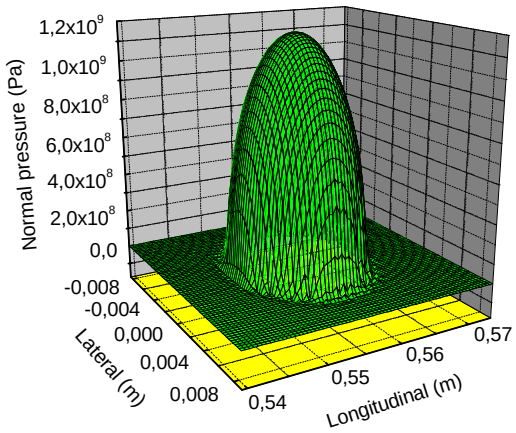

(a) Hertz theory

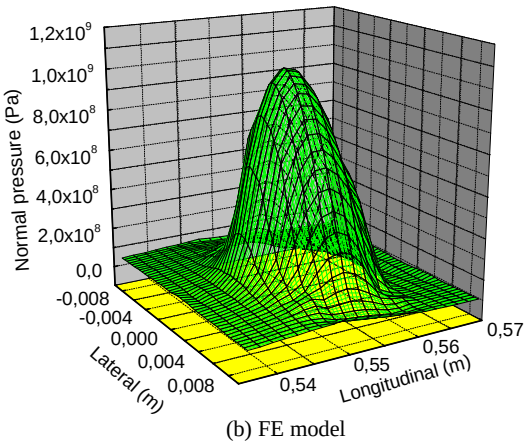

(b) FE model

Fig.5 The normal pressure distribution in the contact patch

For the model used in this paper, the radius of wheel in longitudinal direction is 600 mm, the radius of rail in lateral direction is 300 mm, and the material parameters are shown in Table 1. According to Hertz theory, the values of the semi-

axes of the elliptic contact patch are obtained as: $a = 8.46mm$, $b = 5.26mm$, and the pressure in contact patch is shown in Fig.5 (a).

3.1.2 Comparison

Fig.5 illustrates the comparison of the pressure distribution in the contact patch. It can be seen that the peak got from FE model is slightly lower than that from Hertz theory and the edge of pressure distribution from Hertz theory is much sharper than that from FE model. Those are because the size of rail surface mesh, which is 1.33×1.92 mm in lateral and longitudinal direction of contact plane, compared with the size of contact patch, which is an ellipse with axes lengths 10.52×16.92 mm, is not negligible and one the constant stress element is used. Considering all these factors, it can be concluded that the results from the FE model are in good agreement with those from Hertz theory and the FE model used in this paper is accurate enough.

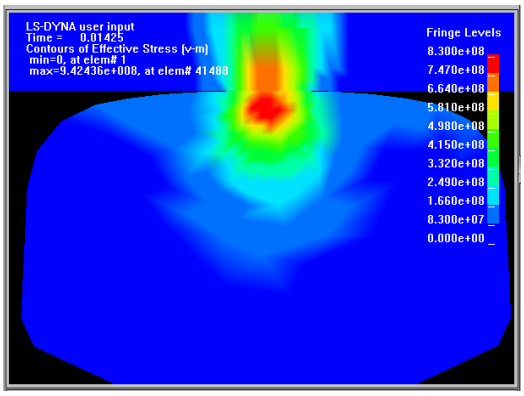

(a) Case 1

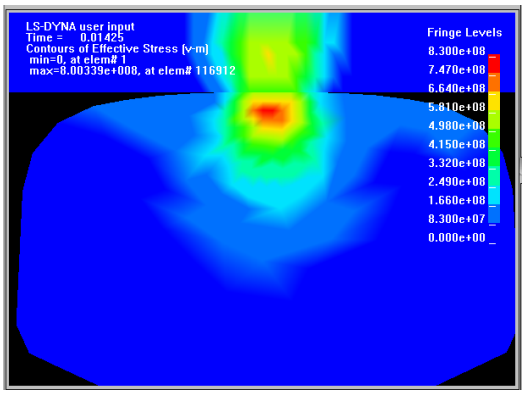

(b) Case 2

Fig.6 The Von Mises stress contours of a rail section

3.2 The effects of tangential contact force

The effects of the tangential contact force can be found by comparing the results of the case 1 and 2. Fig.6 shows the Von Mises stress contours of a rail section that is located in the contact patch at a selected instant (0.01425s). Comparing the two pictures, it can be seen that the stress level of the rail surface in case 1 is higher than that in case 2, but the stress distribution in the sub-surface zone is similar. Particularly in case 1 the maximum stress location is closer to the surface. This means an increasing tangential force will enhance the stress level of the rail surface and may lead to the plastic flow, crack even severe wear of the rail surface material. This coincides with the conclusion of past research: with the increase of friction coefficient, yield begins at the rail surface rather than beneath it [11]. In this paper, rails with smooth contact surface and high yield stress are used, so that no plastic deformation happened.

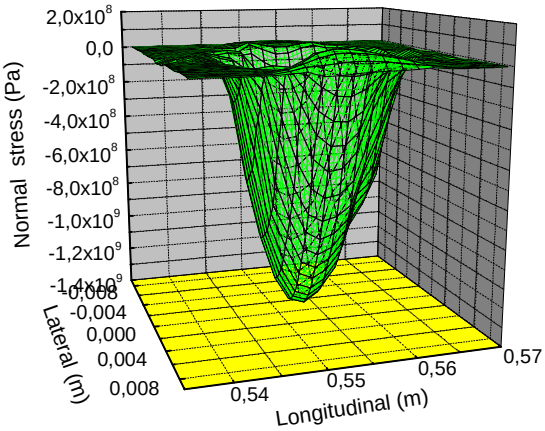

(a) Case 1

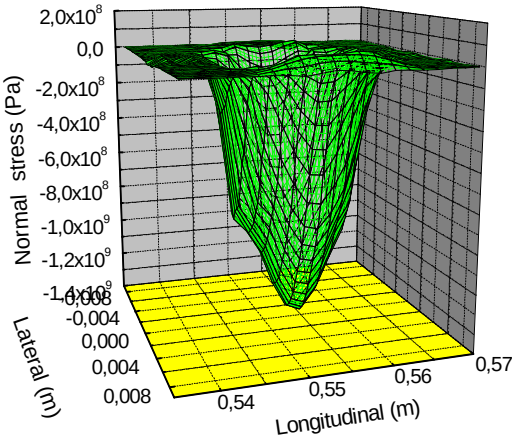

(b) Case 2

Fig.7 The normal stress distribution of the rail surface

With a friction coefficient of 0.3 the maximum stress should already be at or very close to the surface. Close examination of Fig.6 (a) shows that it is not completely the case yet. The reason is that

some error is involved because the constant stress solid element is used and the element size is not infinitesimal. It is also noted that the stress distribution in the wheels is much vaguer. This is again owing to the coarser sub-surface mesh of the wheel.

The 3-D normal and shear stress distributions of the rail surface at time 0.01425s of the two cases are shown in Fig.7 and 8 respectively. The wheel travels different distance at the 0.01425 s in the two cases due to the different acceleration caused by different drive load. And this difference in the two cases is around 0.3 mm. Since the rail is discretely supported in the model, the different contact position can invoke some differences in the normal stress distributions of the two cases. However, the normal stress peaks are almost same in both cases. So it can be deduced that the tangential force in the rolling direction has negligible effects on the normal stress distribution.

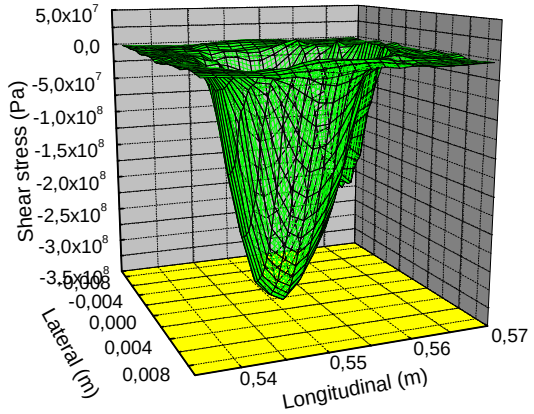

(a) Case 1

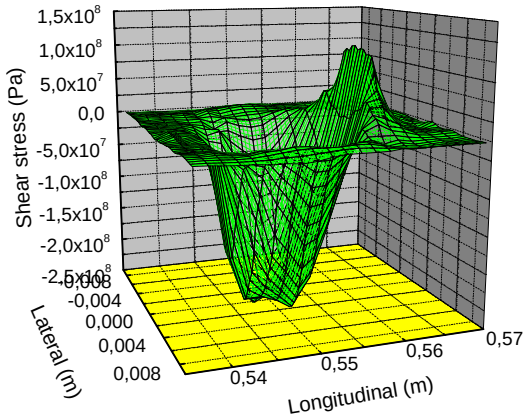

(b) Case 2

Fig.8 The shear stress distribution in rolling direction of rail surface

As mentioned above, the change in tangential force can significantly modify the size of the adhesion area in the contact patch. This can also be seen from the shape and magnitude of the tangential traction distribution that is shown in Fig.8. Comparing with the full sliding contact state (case 1), the shear stress peak of case 2 is reduced by about 30% due to the existence of the adhesion

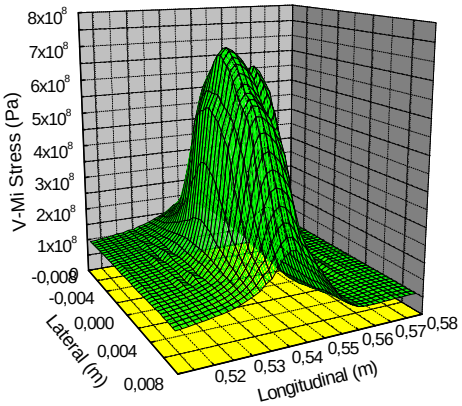

(a) t=0.013965 s

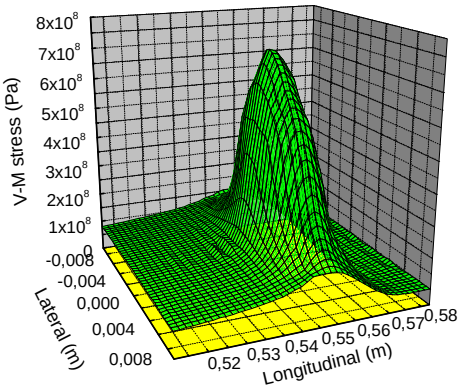

(b) t=0.01425 s

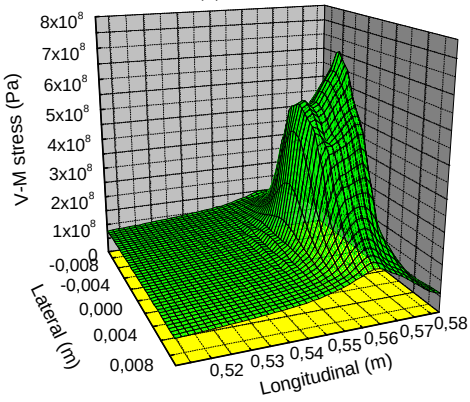

(c) t=0.01435 s

Fig.9 The history of the V-M stress distribution in contact patch

area. It is also noticed that in case 2 the well-known tension area, which is located in the front edge of the contact patch, still exists [15] (see the positive peak in Fig.8 (b)). The reason is that the tangential traction at the leading edge of the

contact in the case 2 is negligible, as illustrated in Fig.4, and the stress state is still dominated by that of a frictionless contact. Nevertheless, for case 1, the tangential traction is already saturated so that the effect of the frictionless normal contact is already submerged. In analyzing these results, the error caused by the one point integration solid element has been taken into account.

3.3 Dynamic effects

Fig.9 illustrates the 3-D rail surface Von Mises stress distribution of the full sliding case (Case 1) at three different instants. It can be noticed that the characteristics of the V-M stress distribution in the contact patch, such as shapes and magnitudes, change with time. That is because those high frequency vibrations of the system are included in the model.

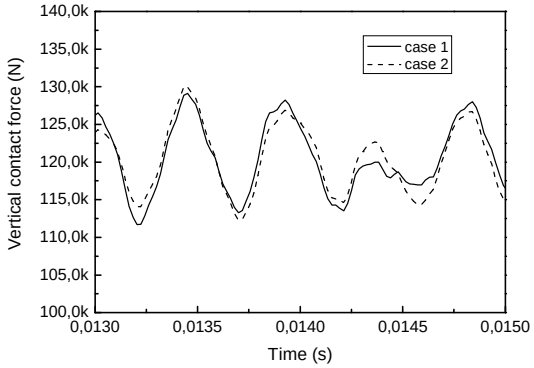

Fig.10 The contact force histories of the two cases

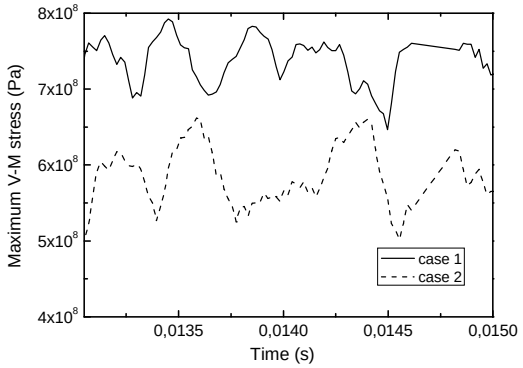

Fig.11 The Max. V-M stress histories of the two cases

The vertical contact force histories of the two cases at a chosen time period are shown in Fig.10. It can be observed that the vertical contact force oscillation is similar in both cases, and around 6.7% of the static load. This is owing to the eigen characteristics of the track-vehicle system. Similar oscillation can also be found in track field observations [13]. Fig.11 presents the maximum V-M stress histories of rail surface elements in the two cases in the same period. It can be found that the oscillating amplitude of maximum V-M stress for case 1, which is 73 MPa (also around 6.7% of the mean value), corresponds to the contact force oscillation in Fig.10. While, for case 2 the oscillating amplitude of maximum V-M stress is 80 MPa (around 11.2% of the mean value). Hence it can be concluded that a rise in tangential force can increase the stress level of the rail surface, but the stress oscillation is higher in the case of lower tangential force.

All results presented in this paper are from the models with smooth rail surface. Based on these results, it is clear that the dynamic response of railway system is significant even in smooth rail condition. In [13], it has been found that the frequency of vertical contact force shown in Fig.10 coincides with the wave pattern of squats. In further works, models with unsmooth rail surface will be studied in order to find the characteristics of dynamic response and stress distribution of squats-type defect.

4 Conclusions

The dynamic stress states of rail surface under frictional wheel/rail rolling contact are investigated in this paper. The FE model employed here can be used to study the rolling contact stress and train states. The contact force frequency and wavelength characteristics agree with track field observations. In the present work, the predicted contact area size and pressure distribution are validated in the quasi-static state against Hertz solution. Based on the results, the following conclusions can be drawn:

1) The tangential force has great influence on the stress state of rail surface. And its increase shifts the maximum shear stress from sub-surface towards surface. This has significant importance for surface initiated rolling contact fatigue.

2) The tangential force has negligible effects on the normal stress distribution, but it can change the shear stress distribution greatly.

3) Even with smooth rail surface, the oscillations of contact force and stress are still significant. And the stress oscillation decreases with the increase of tangential force.

Reference:

[1] F.W. Carter, On the Action of a Locomotive Driving Wheel, *Proceedings of the Royal Society of London*, A112, 1926, pp.151-157.

[2] K.L. Johnson, The Effect of a Tangential Force upon the Rolling Motion of An Elastic Sphere

upon a Plane, *J. Appl. Mech.*, Vol.25, 1958, pp.339-346.

[3] P.J. Vermeulen, K.L. Johnson, Contact of non-Spherical Bodies Transmitting Tangential Forces, *J. Appl. Mech.*, Vol.31, 1964, pp. 338-340.

[4] J.J. Kalker, *Three Dimensional Elastic Bodies in Rolling Contact*, Kluwer Academic Publishers, 1990.

[5] J. Boussinesq, *Application des Potentiels à l'etude de l'équilibre et du mouvement des solides élastiques*, Gauthier-Villars, 1885.

[6] V. Cerruti, *Accademia dei Lincei*, Roma. Mem. fis. mat. , 1882.

[7] Z. Li, *Wheel-Rail Rolling Contact and Its Application to Wear Simulation*, Ph.D Thesis, Technical University of Delft, the Netherlands, 2002.

[8] J Xiaoyu, J Xuesong, Stresses Analysis for Rail/wheel System When Liquid and Micro-roughness existing on contact surface, *Proc. of the 7th International Conference on Contact Mechanics and Wear of Rail/Wheel System*, 24-27 September, 2006, Brisbane Australia, pp. 77-81.

[9] Tao Pang, Manicka Dhanasekar, Dynamic Finite Element Analysis of the Wheel-rail Interaction Adjacent to the Insulated Rail Joints, *Proc. of the 7th International Conference on Contact Mechanics and Wear of Rail/Wheel System*, 24-27 September, 2006, Brisbane Australia, pp. 509-516.

[10] Zefeng Wen, Xuesong Jin, Weihua Zhang, Contact-impact Stress Analysis of Rail Region Using the Dynamic Finite Element Method, *Wear* Vol.258, 2005, pp. 1301-1309.

[11] M. Busquet, L. Baillet, C. Bordreuil, Y. Berthier, 3D Finite Element Investigation on The Plastic Flows of Rolling Contacts —Correlation with Railhead Micro Structural Observations, *Wear* Vol.258, 2005, pp. 1071-1080.

[12] Z. Li, *Correlation Analysis of Squats, Internal project report*, Railway Engineering Group, Technical University of Delft, March, 2006

[13] Z. Li, X. Zhao *et al*, Causes to Squats: Correlation Analysis and Numerical Modeling, *Proc. of the 7th International Conference on Contact Mechanics and Wear of Rail/Wheel System*, 24-27 September, 2006, Brisbane Australia, pp. 439 – 446

[14] A. de Man. *Dynatrack, a Survey of Dynamic Railway Track Properties and Their Quality*, Ph.D Thesis, Technical University of Delft, the Netherlands, 2002.

[15] K.L. Johnson, *Contact Mechanics*, Cambridge University Press, 1985.